This article has been accepted for publication in a future issue of this journal, but has not been fully edited. Content may change prior to final publication. Citation information: DOI 10.1109/JIOT.2021.3050735, IEEE Internet of Things Journal

Multi-cycle testing of commercial coin cells for buffering of harvested energy for the IoT.

James W. Evans, Bernard Kim, Seiya Ono, Ana C. Arias and Paul K. Wright

Abstract— **The sensors and microprocessor-radios of the Internet of Things require power and one possibility is a hybrid source consisting of energy harvesting coupled with a rechargeable battery. This paper concerns a system with a low, but near constant, supply of harvested energy that is sufficient to slowly charge a battery, which buffers that energy and can then supply the higher power level necessary at data transmission. The cycle-life of the battery is then significant and this paper describes the cycling of a commercial lithium coin cell, Panasonic ML2020, for small depth of discharge. Initial work was on a Bio-Logic battery tester and cells were successfully tested, without failure, for a few million cycles at very shallow depth of discharge. Thereafter a battery tester was developed, based on the Particle Photon®, that was much less expensive than a channel of a commercial battery tester. Four cells have been cycled, using this tester, for more than 50 million times with no deterioration in performance evident. Capacitors and a NiMH cell are being similarly tested.**

Index Terms— **battery tester, energy harvesting, IoT, lithium batteries, Panasonic ML2020, secondary batteries.**

I. INTRODUCTION

The ubiquity and growth of the Internet of Things (IoT) are well known. The "nodes" making up the IoT typically consist of a microprocessor connected to one or more sensors and a radio for communication of sensed data to a "gateway" where the data are processed/forwarded/archived. Powering of the nodes is frequently an issue; advances in the electronic components of the node are reducing their size and cost but reducing the size and cost of the power supply proves more challenging. Roundy et al.[1] and, more recently, Raj and Steingart[2] have reviewed the power requirements and availability for IoT motes. The latter authors considered energy storage, distribution (connection to conventional power sources such as a household power socket) and harvesting. Among the energy storage devices considered were primary and secondary (rechargeable) batteries. They concluded that "For consumption of tens of milliwatts or less, power from solar cells or some mechanically-based techniques can be sufficient, but inconsistencies regarding when power is harvested must be balanced by energy storage."

Kim[3] reports on the characteristics and power requirement of several microprocessor-radios and Table I presents the values.

Table I. Characteristics of several microprocessor radios thought to be suitable for the IOT as reported by Kim.

Name (Brand)	Freq [MHz]	TX Current [mA]	TX Power [dBm]	RX Current [mA]	RX Sensitivity [dBm]	Voltage Range [V]
ZL70550 (Microsemi)	779-965 *Sub-GHz*	2.75	-10	2.5	-95	1.71-3.6
ZL70251 (Microsemi)	779-965 *Sub-GHz*	2.4	-11	2.3	-94	1.2-1.9
Simblee (RFDigital)	2400 *BLE*	8	0	10	-93	1.8-3.6
nRF51822 (Nordic)	2400 *BLE*	8	0	9.7	-93	1.8-3.6
nRF8001 (Nordic)	2400 *BLE*	8.4	-18	14.6	-85	1.9-3.6
CC2640 (TI)	2400 *BLE*	6.1	0	5.9	-97	1.8-3.8
BC118 (BlueCreation)	2400 *BLE*	16	7.5	16	-92.5	3.3-4.7
PSoC4 (Cypress)	2400 *BLE*	16.5	0	18.7	-92	1.71-5.5
DA14580 (Dialog)	2400 *BLE*	4.9	0	4.9	-93	0.9-3.6
STM-300U (Enocean)	902 *Sub-GHz*	24	5.5	33	-98	2.6-4.5
SPSGRF (ST)	915 *Sub-GHz*	9	-7	10	-118	1.8-3.6
MKW01Z128 (NXP)	315-955 *Sub-GHz*	20	0	16	-120	1.8-3.6
nRF905 (Nordic)	433-915 *Sub-GHz*	9	-10	12.5	-100	1.9-3.6
CC1310 (TI)	315-920 *Sub-GHz*	12.9	-10	5.5	-124	1.8-3.6
CC430xx (TI)	315-915 *Sub-GHz*	15	0	15.4	-112	1.8-3.6
Si4455 (Silicon Labs)	284-960 *Sub-GHz*	18	10	10	-116	1.8-3.6

It is seen that of the order of 10mA are required for both transmission and receiving of data. Fig. 1 shows measurements at Berkeley of the current drawn by a Nordic Semiconductor® development board during sleep, data acquisition and transmission[4]. Power requirements when the mote is in a sleep state are minimal; power requirements when acquiring data from sensors are sensor dependent but usually less than the TX/RX requirements. It would appear that the hybrid system of energy harvesting and storage, implied by the quotation above, must be designed to take care of fluctuating power *demand*, as well as fluctuating supply from the harvester.

James W. Evans is Professor of the Graduate School, Dept. of Materials Science and Engineering, University of California, Berkeley, Ca 94720 (evans@berkeley.edu).

Bernard Kim, Ph.D. recipient from Dept. of Mechanical Engineering, UC, Berkeley, is a Reliability Engineer at Apple, Inc. (bernard.kim@berkeley.edu).

Seiya Ono is an MS student in the Dept. of EECS, UC, Berkeley.

Ana C. Arias is Professor, Dept. of EECS, UC, Berkeley. (acarias@berkeley.edu).

Paul K. Wright is Professor Emeritus, Dept. of Mechanical Engineering, UC, Berkeley (pwright@berkeley.edu).

This article has been accepted for publication in a future issue of this journal, but has not been fully edited. Content may change prior to final publication. Citation information: DOI 10.1109/JIOT.2021.3050735, IEEE Internet of Things Journal

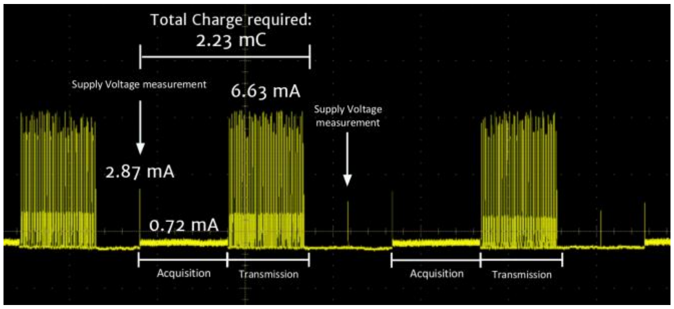

Fig. 1. Current drawn by a Nordic Semiconductor® development board as it acquires and transmits data, then sleeps. The period covered is approximately three seconds.

The present investigation arose from a proposal to deploy nodes in a data center where a 20 mm diameter micro-wind turbine (MWT)[5], running off cooling air flow, would be the primary source of energy and would store energy in a secondary battery. Hundreds of such nodes would be deployed and would report data (principally air temperature) at 30 minute intervals. Data transmission was anticipated to require 10mA and ~140ms from the battery, with the other energy requirements provided directly by the MWT. After each transmission, the battery would then be recharged over 30 minutes. The choice for the secondary batteries was a commercial lithium coin cell to be consistent with the size of the MWT. Because of the hundreds of nodes and the desire to minimize maintenance, the question arose as to whether the coin cells could withstand cycling for a period of a few years, i.e. for a few million cycles. To address this question in a reasonable time period, it was reasoned that the cells would be more stressed if they were recharged in a period of a few hundreds of milliseconds, rather than in 30 minutes, thereby an accelerated testing could be carried out where a few discharge/recharge cycles would occur each second. Were the cells to achieve a few million cycles in this way, there would be reasonable confidence in a lifetime of a few years in practice. Accelerated testing was first carried out on a commercial battery tester. However, even when accelerated, the testing consumed an inconvenient time on a tester that was in demand for other projects. Hence, an inexpensive circuit based on the Particle Photon® was developed and used for much of the investigation.

II. EXPERIMENTAL METHODS

Initial experiments were carried out on Panasonic ML2020 coin cells using a Bio-Logic BCS-810 battery tester. This cell is 20mm diameter by 2mm. It has a lithium/aluminum alloy as the negative electrode and a compound manganese oxide positive electrode. The cells are rated for one thousand discharge/charge cycles at 10% depth of discharge. No deliberate process was entailed in selecting the ML2020; a supply was available in our lab. Cells, which have a nominal capacity of 45mAh, were first tested at constant current discharge ranging from 0.2 to 2mA until 40mAh of discharge. Results from such testing were unremarkable and in accord with the manufacturer's literature[6] so they were not included below. New cells were then subjected to one of two kinds of cycling:

- Deep cycling where cells were discharged at 10mA down to 2V before recharging at 1mA.
- Shallow cycling where cells were discharged with a 10mA current for 0.132, 0.660, or 1.32s. Cells were then recharged with a constant current of 10mA until 3.2V was reached or for 13.2s, whichever occurred first.

Details concerning this phase of the investigation are in Kim's dissertation[3].

Commercial battery testers cost a few thousand dollars per channel. In order to make testing at lower cost possible, and thereby to make it feasible to test many batteries simultaneously, we devised a circuit based on the Photon®. This microprocessor-radio is similar to the well-known Arduino with two important differences:

- the Photon® communicates wirelessly so that software changes and data acquisition can be achieved remotely
- the Photon® has a true DAC output (as opposed to a pulse width modulation output) that can handle both positive and negative currents.

The cell cycling circuit is shown schematically in Fig. 2 and its simplicity leads to a total cost, including the Photon®, of a few tens of dollars.

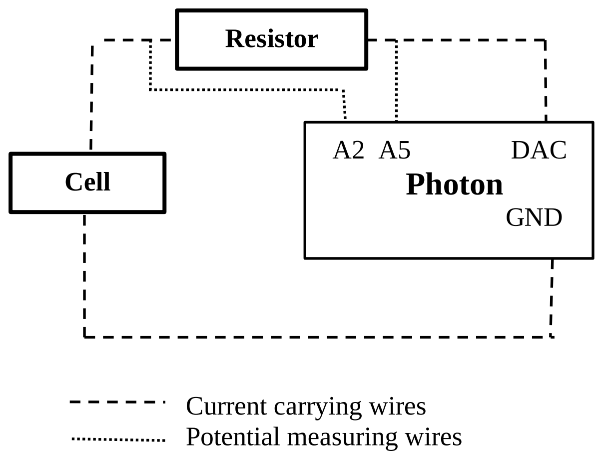

Fig. 2. Schematic of the Photon®-based circuit for testing cells.

On cell charging, the DAC output drives current through the cell via a 10 ohm resistor; on discharging the cell reverses the current from the DAC. Connections from the resistor to the analog inputs of the Photon® yield the cell voltage (A2) and the voltage across the resistor (A5-A2) and thereby the current. The code written for this application included a control algorithm with both proportional and integral action so as to maintain a specified (10mA) current during discharge by manipulating the DAC. The integral was periodically set to zero to avoid "integral wind-up" and this led to brief perturbations of the current from 10mA that are seen in section III. Recharging was at a constant DAC output to a specified final voltage of 2.2V in ~150ms. That voltage is below the recharge capabilities of the ML2020 but the DAC output (nominally up to 3.3V) was unable to drive the cell to higher voltages in reasonable time. Fig. 3 gives more details of the circuit.

This article has been accepted for publication in a future issue of this journal, but has not been fully edited. Content may change prior to final publication. Citation information: DOI 10.1109/JIOT.2021.3050735, IEEE Internet of Things Journal

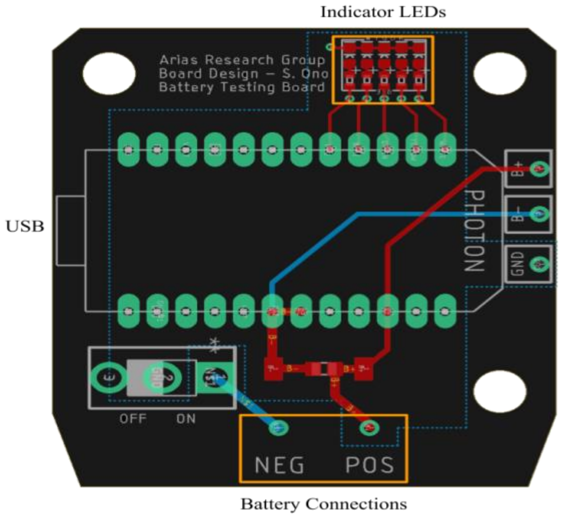

Fig, 3. Layout of the battery testing board. Terminals for connecting the cell are on the bottom, adjacent to the on-off switch. The resistor is just above those terminals. Terminals on the right allow for external measurement of current and voltage, for example in the Arduino/Tera Term measurements of Fig. 8. LEDs on the top right allow signaling of the operation of the board (e.g. charging) as controlled by the code on the Photon®. The USB connection for power is on the left. The board measures 46mm by 51mm.

The data from the Photon® were transmitted by the local network to the ThingSpeak® cloud of MathWorks® for further processing using MATLAB®.

In an auxiliary experiment, the rapid changes in voltage and current of the ML2020, during cycling on the Photon®-based circuit, were captured using an Arduino and Tera Term® software, generating a CSV file of these two variables over a few seconds for plotting.

III. EXPERIMENTAL RESULTS

The effect of cycling the ML2020 cell for 100 cycles is shown in Fig. 4. The cell was discharged from 3.2V to 2.0V at 10mA and then recharged at 1mA. Clearly this order of cycling causes the cell to significantly lose performance over only a hundred cycles. These discharges of 18-29% of the cell nominal capacity are much deeper than the discharges of the cycling described below and will be contrasted with the latter cycling results in section IV.

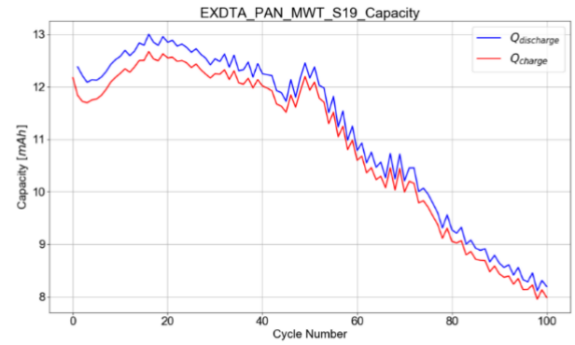

Fig. 4. Deterioration of the capacity of an ML2020 after discharge cycling by 18-29% of nominal capacity.

Fig. 5 shows the results from the Bio-Logic tester when five cells were cycled by discharging at 10mA for the time interval specified in the legend, followed by charging at 10mA back to 3.2V. The vertical axis is the voltage at the end of discharge; the inset shows the voltage during cycling a cell with a 660ms discharge. Note that, in contrast to the cell of Fig. 4, the cells reach a few million cycles. Subsequent results are from the Photon®-based tester.

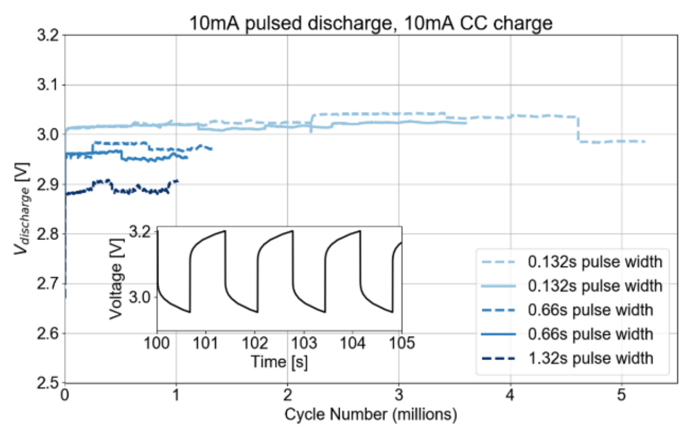

Fig. 5. Cycling of ML2020 cells on the Bio-Logic tester.

Four ML2020 cells were started on Photon®-based testers in mid-September, 2019. The cycling was suspended from October 8th to October 30th and there were additional, but brief, interruptions of power or internet connectivity later that year and in 2020. The data presented in Fig. 6 are for one of these cells started on September 8th and encompass more than 50 million cycles to April 20th, 2020. The other three cells have shown similar performance and achieved a similar number of cycles. Shown are the voltages at the beginning and end of the 10mA discharge of 140ms. The spikes are due to the perturbation from resetting of the integral control mentioned in section II. There is a periodic variation of ~50-100mV with a period of ~230,000 cycles which probably results from diurnal variation in the temperature of the room. The insets, at ~30 million cycles, show the voltages at finer resolution and the diurnal variation is visible in the one at lower left..

This article has been accepted for publication in a future issue of this journal, but has not been fully edited. Content may change prior to final publication. Citation information: DOI 10.1109/JIOT.2021.3050735, IEEE Internet of Things Journal

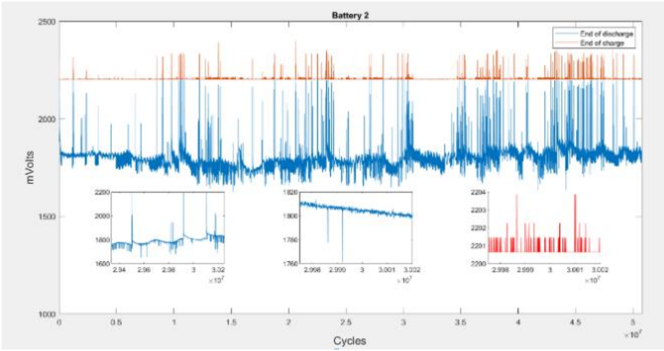

Fig. 6. Voltage traces for an ML2020 tested over 50 million cycles. The insets are at ~30 million cycles.

The corresponding current, averaged over each discharge is displayed in Fig. 7. Again, the spikes in current are the result of resetting the integral action of the control algorithm. The inset shows that the control algorithm gives a satisfactory control of discharge current.

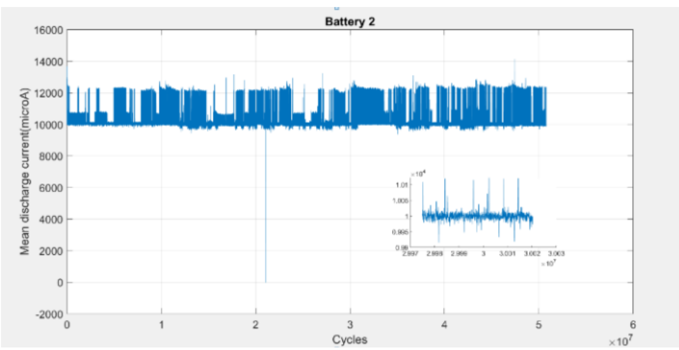

Fig. 7. Current trace for an ML2020 tested over 50 million cycles. The inset is at ~30 million cycles.

Fig. 8 shows the results from the Arduino/Tera Term measurements over a few cycles near 30 million cycles. The Photon®-based circuit is seen to be correctly varying the voltage in the way seen (inset of Fig. 5) for the Bio-Logic tester. The voltage drop of ~200mV that is from the end of charging to the end of discharging, lies within the range that many microprocessors could accommodate (last column of Table I)

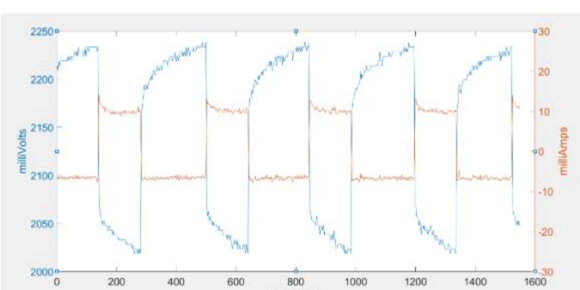

Fig. 8. Cell voltage and current measured by the Arduino/Tera Term, applied to terminals on the Photon®-based circuit, near 30 million cycles.

IV. DISCUSSION

The results of the cycling displayed in Figs. 5-8 are in contrast to those of Fig. 4. They should also be contrasted to the cycle life claimed by the manufacturer: the cells are rated for one thousand cycles at 10% depth of discharge. These contrasts are because the results of the present investigation are for a very low extent of discharge; for a nominal 45mAh cell discharged at 10mA for 140ms, the incremental depth of discharge is only 0.00086% versus the 18-29% of Figure 4. Nevertheless, the former cells have each had discharges summing to 432 times their nominal capacity of 45mAh when they reach 50 million cycles. None of the four cells has failed and the relatively small changes over 50 million cycles evident in Figs. 6 & 7 suggest that little electrochemistry has happened in these cells. A plausible hypothesis is that the cells are functioning as capacitors with surface phenomena, rather than electrochemical phase change, or intercalation which would affect the electrodes, taking place.

It is likely that a supercapacitor could achieve the cycle life of the ML2020 but a cell does have the advantage of being able to cope with longer discharge periods if, for example, the nodes were powered by a solar cell. The manufacturer of the ML2020 claims a self-discharge rate of only 2% per year at 20^0C.

The Photon®-based circuit has proved itself to be an inexpensive device for testing batteries, although lacking the ability to rapidly charge to much above 2.2V. It is also challenging to make the device measure an open circuit potential, which commercial testers can do. The C code of this application has maintained a constant current discharge and a constant current charge (Fig. 8) but can be readily changed to a different protocol, for example one where variations of charging current are superimposed to simulate energy harvesting from a solar panel.

The Photon®-based circuit may be compared to the Jonny Galvo of Steingart and colleagues[7], which employed an Arduino, or to the ABE-Stat of Jenkins et al. which used a custom circuit[8]. The latter is a more sophisticated device that functions as a potentiostat and is capable of such electrochemical techniques as impedance spectroscopy. Jenkins et al. include a table of other custom potentiostats in their paper. Another, recently described, open-source potentiostat is that of Ainla et al.[9] These investigators developed a Universal Wireless Electrochemical Detector that communicates with the internet via a smart phone.

At time of preparation of the manuscript, the four ML2020 cells continue to cycle with no deterioration in their performance evident. A Varta NiMH coin cell and two supercapacitors are also under test using the Photon®-based circuit. The NiMH cell has passed eight million cycles on the same charge/discharge schedule as the ML2020s.

Lithium containing cells are known to pose a risk of thermal instability (e.g. Song and Evans[10]) and might therefore be thought unsuitable where fire hazards are unacceptable. The ML2020 has a large surface to volume ratio and contains only a small amount of lithium (more correctly a lithium-aluminum alloy) so that the danger of thermal excursion is low. Nevertheless, it might be appropriate to mount the cell on heat sinks. One concept is to contact alumina discs, of the same diameter as the cell (20mm), on the top and bottom of the cell to serve as such sinks. The most likely cause of a thermal excursion is the exothermic reaction between the lithium of the anode and the manganese dioxide cathode:

$$4Li + MnO_2 = 2Li_2O + Mn$$

for which the enthalpy of reaction, available from thermodynamic tables, varies from -168.9kJ/mol Li at 300K to -167.3kJ/mol Li at 460K (just above the melting point of lithium). The quantity of lithium in the ML2020 can be estimated from the cell capacity, using Faraday's law, and is 1.7×10^{-3} mol. Thus heat released by the above reaction is 284J to 281J. Supposing 5mm thick discs of alumina as heat sinks, and using the heat capacity and density of alumina, 0.88J/(g.K) and 4.0g/cm^3, the temperature increase of the alumina discs, if they capture all the heat of reaction, is between 25 and 26K which might be acceptable, depending on the application. This calculation should be regarded as a first approximation and a more careful analysis would be required before it can be concluded that alumina heat sinks are fit for purpose. The analysis would examine the possibility that the cell contains excess lithium (beyond that needed to supply the nominal 45mAh); that the aluminum of the alloy anode could also react with the cathode, and that heat transfer from cell to the alumina discs would be imperfect

REFERENCES

[1] Shad Roundy, Daniel Steingart, Luc Frechette, Paul Wright and Jan Rabaey, "Power Sources for Wireless Sensor Networks", Wireless Sensor Networks, 1, 2004.

[2] Abhi Raj and Daniel Steingart, "Review – Power Sources for the Internet of Things", J. of the Electrochem. Soc., 165 (8) B3130-B3136, 20018.

[3] Bernard Kim, Ph.D. dissertation, "Optimization and Characterization of a Layer-by-Layer, Fully Printed, Secondary Zn-MnO2 Battery with an Ionic Liquid Gel Polymer Electrolyte for Internet of Things Applications", December, 2019.

[4] Pierluigi Raffone, MS Thesis, "Printed Self-Powered Wireless Sensor Node for Ubiquitous Computing ", Politecnico di Milano, 2015-16.

5 David A. Howey, Anshu Bansal and Andrew S. Holmes , "Design and Performance of a Centimetre-scale Shrouded Wind Turbine for Energy Harvesting", Smart Materials and Structures, 20, paper 085021 (12pp), 2011.

[6] https://batteries.eu.panasonic.com/batteryfinder/v3.0/_pdfs/Lithium-Handbook.pdf June, 2020.

[7] Daniel Steingart, Alex Redfern, Christine Ho, James W. Evans and Paul K. Wright, "Jonny Galvo: A Small, Low Cost Wireless Galvanostat", ECS Transactions, 1 (21) 17-22, 2006.

[8] Daniel M. Jenkins, Bog Eum Lee, Soojin Jun, José Reyes-de-Corcuera and Eric S. McLamore, "ABE-Stat, a Fully Open-Source and Versatile Potentiostat Project Including Electrochemical Impedance Spectroscopy." J. of the Electrochem. Soc., 166 (9) B3056-B3065, 2019.

[9] Alar Ainla, Maral P. S. Mousavi, Maria-Nefeli Tsaloglou, Jula Redston, Jeffrey C. Bell, M. Teresa Fernández-Abedu and George M. Whitesides, "Open Source Potentiostat for Wireless Electrochemical Detection with Smart Phones", Analytical Chem. 90, 6240-6246, 2018.

[10] Li Song and James W. Evans, "The Thermal Stability of Lithium-Polymer Batteries", J. Electrochem. Soc., 145, 2327-2334, 1998